

The Characteristics of Cutting Force in the Rough Machining Process of 5-Axis Milling on PEEK Material Based on Cutting Speed Parameters

Himawan Hadi Sutrisno

Fire, Material and Safety Laboratory, Universitas Negeri Jakarta, Indonesia

Email: Himawan-hadi@unj.ac.id

Abstract—This study determines the cutting force characteristics of the 5-axis milling rough machining process based on the differences in cutting speed, especially on composite materials. The data generated are useful for operators in the machining process in the manufacturing industry. Simulations and experimental methods are used, and data generated from cutting force sensors are validated using mathematical models commonly used for cutting force calculations. From the obtained data, the characteristics of the cutting force influenced by the cutting speed of the machining process are further analysed. The material is a PEEK composite used by the manufacturing industry. The tool used is a material-type high-speed tool steel end mill. By using a machine-type table tilting 5-axis mill for the rough machining process, the variation in cutting speed affects the tool cutting force at each shear angle. The data showed that the lowest cutting speed produces a high cutting force on the x-axis component. In this component, the largest value is 39.73 N at a cutting speed of 18.84 m/min; at the y-axis at the same cutting speed, the largest cutting force value is 79.20 N. The z-axis component value is 16,405 N, which exhibits the lowest cut force value compared to the increase in the speed of the other cuts used in the study. The increase in tool cutting speed does not always increase the cutting force of each machining axis.

Index Terms—5-axis machining, cutting force, cutting speed, PEEK, rough machining

I. INTRODUCTION

Machining process is an important part of the production of goods in the manufacturing industry; however, the work piece model that can be produced excessively by the machining process is complex. To support this fact, machine manufacturers try to improve the quality of the machines produced to meet industry demands so that the quality and capabilities of operators are also increased. The complexity of the work piece in terms of materials used in the manufacturing industry is also experiencing considerable development. In the last decade, automotive products and the aircraft industry have abandoned using aluminium and metal materials and have switched to using carbon fibre; this material provides several advantages over metals. However, the

machining process that uses raw materials other than metal is highly dependent on the machinability characteristics of the material itself. This feature is based on the fact that differences in the composition of composite materials produce different characteristics of mechanical properties [1–4].

All machine operators in the manufacturing industry must immediately adjust to this trend. The machining process is generally divided into two parts: the rough machining process and the finishing machining process. In the rough machining process, the effectiveness of the production process becomes highly decisive because forming a work piece near the finished form takes time, which has implications for the effectiveness of the production process on an item; thus, the effectiveness of the rough machining process has an important role in determining the cost of production [5–7]. Consequently, machining parameters are often used as optimal means to increase the effectiveness of the machining process. For example, cutting speed is added during the production process so that the machining time becomes slightly faster.

The determination of the parameters of this machining process is highly dependent on the operator of the machine itself. If the machining parameters are changed just to increase the machining process, the work pieces or tools are often damaged because the resulting cutting force is too large to the detriment of the manufacturer [8]. Regarding cutting force research, Matsumura et al. [9] revealed that the use of a large cutting force during the machining process affects the load received by the tools and produces different chips, as well as results in differences in the style received by the tool itself and affects the time of the tools. However, raw materials used, such as composite materials, also affect the machining process. The magnitude of the tool cutting force is generally examined by an experimentally derived dynamometer, where the data obtained from the actual machining process are used to determine the coefficient of the cutting force [10]. The data of this experiment are then used as a calculation of the cut force coefficient in a mathematical model [11–15].

By calculating the cutting force using the model, Braun et al. [8] revealed that the chip formation of the machining process is influenced by the shear angle plane

on orthogonal cutting. The shear angle is used to determine the cutting force depending on the tool parameters and the material used in the simulation process [16–19]. According to Schwenzer et al. [11], the modelling of the cutting force in machining processes can use the Kienzle–Viktor empirical formula, where the feedback from the actual force load received by the tool on the spindle is connected to the tool trajectory resulting from the CAM system, which determines the mechanistic cutting force.

The coefficient of the cutting force obtained depends on the tool and material parameters used [20, 21]. In addition to metals, carbon fibre composite materials are trending in cutting force research. According to Wan et al. [22], this material is growing rapidly and is also influenced by the direction of carbon fibre itself. Their review papers involve a carbon fibre direction that is perpendicular to the direction of the machining process, resulting in a high cutting force, which is derived from experimental and mathematical calculation results. According to He et al. [23], the experimental data showed that one tool trajectory in the form of slot milling exhibits a difference in cutting edge position and fibre orientation angle, which affects the difference in the size of cutting force. This finding is in accordance with the research of Parhad et al. [24]. They showed the changes in machining parameters by increasing the value of cutting speed, which reduces the cutting force. However, when the depth of the cut value is added, the cutting force increases [25].

Based on the description above, even though research has revealed the relationship of machining parameters to the magnitude of the cutting force and their effects on the lifespan of tools, operators still use several rapid ways by changing the feed rate online during the machining process to accelerate the production process. This factor is based on the understanding that when the set machining parameters are changed to a certain speed that is still within the safe limit, damage to tools then does not occur. From a series of experiments performed in this study, the phenomenon of large changes in cutting force is observed, which is affected by changes in the cutting speed of machining parameters, especially in PEEK composite materials. The collected data show that the large difference in cutting force against the large difference in cutting speed of the machining process, especially the PEEK composite material, is used as a reference material for operators and implies that tool damage can be avoided.

II. METHODS

This research uses an experimental and simulation method. After the materials and equipment are properly prepared, the results of the real cutting force measurements are compared with the cutting force modelling that has been currently developed.

A. Material and Machine Preparation

The tool used in this research is the high-speed tool steel flat end mill 4 flutes, with a tool diameter of 10 mm,

a tool radius of 5 mm, a shank diameter of 10 mm and a tool length of 70 mm. This tool is mounted on a 5-axis milling machine with a table tilting type. The work piece and force-measuring tool installation used are shown in Fig. 1. The tool path is made using a cut value with a constant depth by the 3-axis rough milling method. By using the CAM software, the tool path used in this study is shown in Fig. 2, and the machining parameters are provided in Table I.

After the NC file can be created, the Zig method is selected to facilitate the observation and retrieval of cutting force data at any time.



Figure 1. Installation of work pieces and force-measuring tools in the machining process

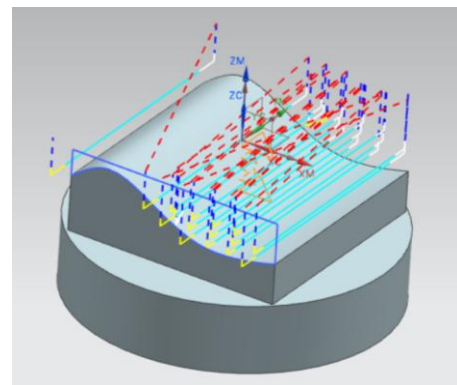


Figure 2. Tool path of the initial machining process

TABLE I. PARAMETERS OF ROUGH MACHINING PROCESS

No	Parameters	Annotation
1	Cutting Speed	(18.84 m/min) (21.98 m/min) (25.12 m/min) (28.26 m/min) (31.40 m/min)
2	Feed Rate	0.05 mm/tooth
3	Depth of Cut	5 mm

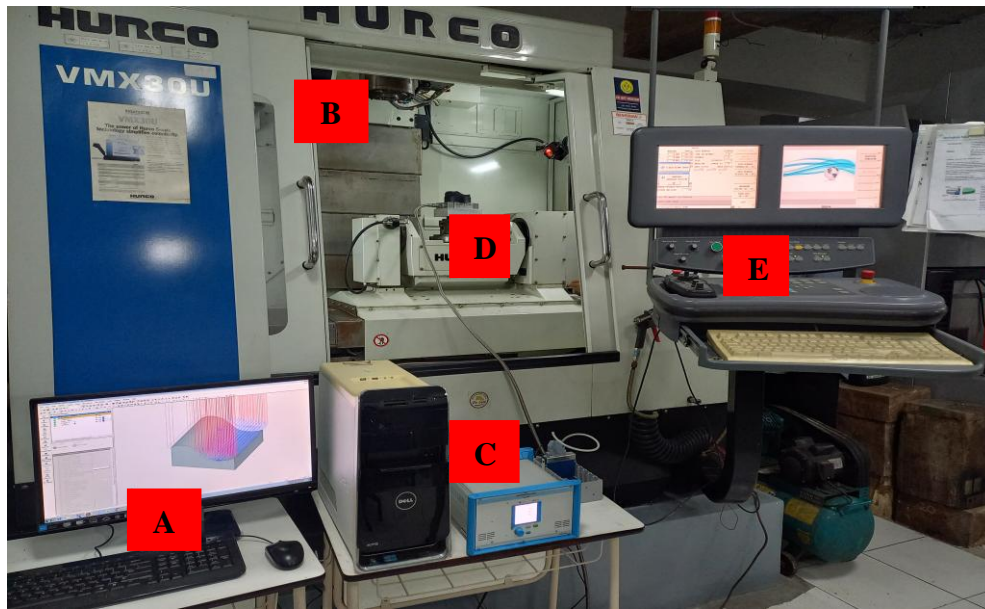
From the machining parameter table shown above, a constant 5-mm deep cut is used, and five cutting speed variations are used, which are obtained from the

difference in spindle speed set in the CAM software to produce the NC files. The material used for this research is the PEEK composite material. This material decomposes at 426 °C based on the results of thermogravimetry analysis test

B. Experimental Setup

The work piece is mounted on a Kistler-type 9192A dynamometer that is also mounted on an amplifier. The

amplifier is then connected to the data acquisition NI9201C series module and plugged into an Ethernet chassis NI cDAQ 9188. This module functions as a data acquisition device that sends pulses from the amplifier into data that can be stored on the monitor screen. The procedure for installing the data acquisition module in this study is shown in Fig. 3.



Cutting force data collection

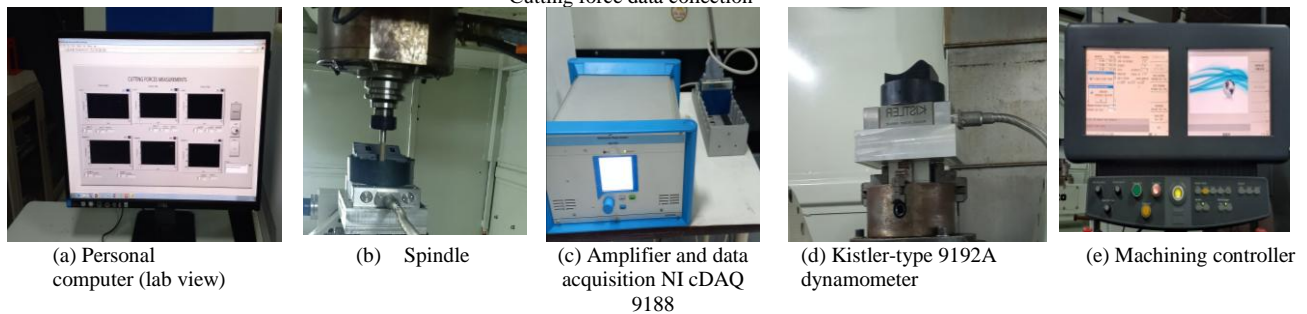


Figure 3. Experimental procedure

From the material characteristics mentioned in the rough machining process, the strain caused by the tool on the material used may occur. It can produce vibrations and affect the changes in cutting forces. However, this effect can be eliminated by taking the cutting force data more than once; thus, errors due to vibrations can be avoided.

From the abovementioned testing stages, data are collected from the machining process every second at a rate of 100 data per second. From this 100 data/second, the tool rotation angle can be determined and used to calculate the cutting force.

As conducted by Rubeo et al. [26], the cutting force can be calculated by considering the tangential (f_t), radial (f_r) and axial (f_a) forces, as well as the friction and shear angles. The f_t , f_r and f_a occur during tool penetration, and the cutting force can use Equation (1):

$$\begin{bmatrix} F_x \\ F_y \\ F_z \end{bmatrix} = \begin{bmatrix} \cos\theta & \sin\theta & 0 \\ \sin\theta & -\cos\theta & 0 \\ 0 & 0 & 1 \end{bmatrix} \begin{bmatrix} F_t \\ F_r \\ F_a \end{bmatrix} \quad (1)$$

To calculate the f_t , f_r and f_a in the machining process, Equations (2), (3) and (4) can be used:

$$F_t = K_{tc}bh + F_{cp} \quad (2)$$

$$F_r = K_{rc}bh + F_{tp} \quad (3)$$

$$F_a = K_{ac}bh + F_{ae}\Delta y \quad (4)$$

where b is the nominal cut width, and h is the nominal cut thickness. F_{cp} is the factor for approximating the effect of different rake angles on the cutting force. F_{ip} is the factor for approximating the effect of different cutting edge inclination angles. F_{ae} is the factor for approximating the effect of the width of land wear on the cutting forces in this process. F_{ae} is rated 0 or none at all because the value is minor. F_{cp} , F_{ip} and F_{ae} are the average forces from every cutting data in the tool coordinates that can be calculated from the measured maximal and minimal forces in the machine tool coordinates.

K_{tc} is the coefficient of the tangential cutting force. K_{rc} is the coefficient of the radial cutting force. K_{ac} is the coefficient of the axial cutting force. To calculate the coefficients of these cutting forces, we used Equations (5), (6) and (7):

$$K_{tc} = \frac{\tau}{\sin \phi_n} \frac{\cos(\beta_n - \alpha_n) + \tan i \tan \eta \sin \beta_n}{\sqrt{\cos^2(\phi_n + \beta_n - \alpha_n) + \tan^2 \eta \sin^2 \beta_n}} \quad (5)$$

$$K_{rc} = \frac{\tau}{\sin \phi_n} \frac{\cos(\beta_n - \alpha_n) \tan i - \tan \eta \sin \beta_n}{\sqrt{\cos^2(\phi_n + \beta_n - \alpha_n) + \tan^2 \eta \sin^2 \beta_n}} \quad (6)$$

$$K_{ac} = \frac{\tau}{\sin \phi_n} \frac{\sin(\beta_n - \alpha_n)}{\cos i \sqrt{\cos^2(\phi_n + \beta_n - \alpha_n) + \tan^2 \eta \sin^2 \beta_n}} \quad (7)$$

Furthermore, the tool position and shear angle are calculated using Equations (8) and (9), respectively. The chip compression ratios are set using Equation (10):

$$\tan \beta_n = \tan \beta \cos \eta_c \quad (8)$$

$$\phi_n = \tan^{-1} \frac{r_c \cos \alpha_r}{1 - r_c \sin \alpha_r} \quad (9)$$

$$r_c = \frac{h}{h_c} \quad (10)$$

In calculating the chip compression ratio (r_c), the chip thickness (h) can be calculated using Equation (11):

$$h = c \times \sin \theta \quad (11)$$

The feed rate for each tool angle (c) can be calculated using Equation (12):

$$c = f_z \times z \quad (12)$$

III. RESULTS AND DISCUSSION

A. Validation Data

At a spindle rotation of 600 rpm, the cutting speed is 18.84 m/min, and feed per tooth (f_z) = 0.05 mm/tooth, the

data storage system of the data acquisition tool can be set to save every 100 data per second so that each recorded data has a 0.01-second time difference. This feature equates to 10 laps/second; thus, it would equal to 10 revolutions per 100 data. From the 300 data collected in the first second (first 100 data), the cutting force has fluctuating values; however, after the first, second or so 100 data, the cutting force data generated from the machining process have experienced stability. From the diversity of the second or so data, the validation process is conducted to determine the characteristics of the cutting force that was generated from the experiment.

From the mathematical model that is commonly used when the tool rotates and produces 1 data, the chip thickness, chip compression ratio and shear angle on the work piece are as follows (Table II):

TABLE II. CHIP THICKNESS, CHIP COMPRESSION RATIO AND SHEAR ANGLE

Θ°	Chip Thickness (mm)	Chip Compression Ratio	Shear Angle
0	0	0	0
36	0,11755705	1,67938644	66,81384985
72	0,190211303	2,71730433	78,83547544
108	0,190211303	2,71730433	78,83547544
144	0,11755705	1,67938644	66,81384985
180	2,4503E-17	3,5004E-16	1,97513E-14

After obtaining the chip thickness value, chip compression ratio and shear angle, the cutting force coefficients K_{ac} , K_{tc} and K_{rc} are shown in Table III.

TABLE III. COEFFICIENT OF CUTTING FORCE K_{ac} , K_{tc} AND K_{rc}

Θ	K_{tc}	K_{ac}	K_{rc}
0	0	0	0
36	105,316546	22,92254798	33,27061034
72	132,2575015	28,78634972	41,78154301
108	132,2575015	28,78634972	41,78154301
144	105,316546	22,92254798	33,27061034
180	8,1448E+16	1,77275E+16	2,57303E+16

After the cutting force coefficients K_{ac} , K_{tc} and K_{rc} are determined, the instantaneous cutting force can be calculated, and the cutting force at each turn of the tool angle can be determined. Table IV shows the instantaneous cutting force and the magnitude of the cutting force that occurred at each turning angle of the tool.

TABLE IV. INSTANTANEOUS CUTTING FORCE AND SIZE OF CUTTING FORCE

Θ	Instantaneous Cutting Force (N)		
	F_t	F_a	F_r
0	0,0349416	0	0,089799912
36	37,17704913	8,08412139	11,82338437
72	75,50555676	16,42646729	23,93176516
108	75,50555676	16,42646729	23,93176516
144	37,17704913	8,08412139	11,82338437
180	6,022098336	1,303127503	1,981206024

From the number of turns of the tool every second, the angle of rotation in each resulting data can be determined, which is 36° per recorded data from the experiment carried out for 3 seconds or consisting of 300 large data on the cutting forces on the x-axis (F_x), y-axis (F_y) and z-axis (F_z).

The resulting cutting force is then compared with the results of the calculations presented in Table V. At each angle, the tool produces a cutting force value on the F_x ,

F_y and F_z components. Here, they are then all recorded signals in the machining process, which last for the first 3 seconds (Fig. 4).

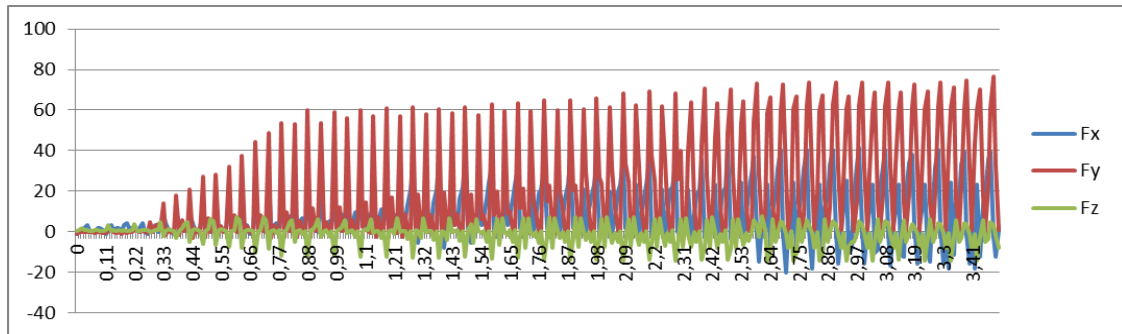
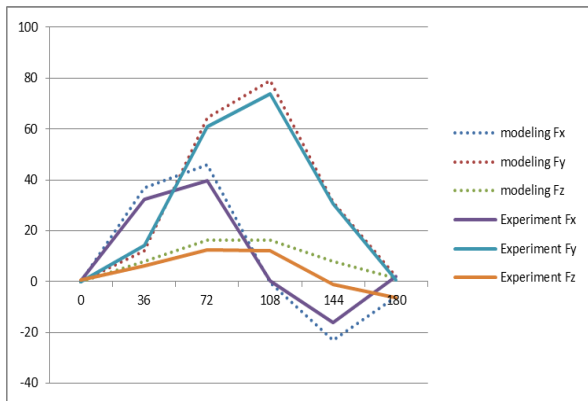


Figure 4. Cutting force signal for first 3 seconds.

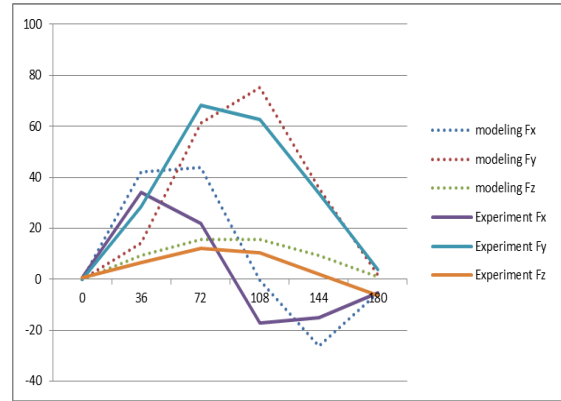
The comparison of the cutting force graph at each rotation angle of the tool from both the experimental and simulation results is shown in Fig. 5, where the modelling results performed and the actual data obtained have the same characteristics. This finding shows that the model employed and the data generated from the experiment can be used to obtain the characteristics of the cutting force at any difference in tool cutting speed.

TABLE V. CUTTING FORCE (N)

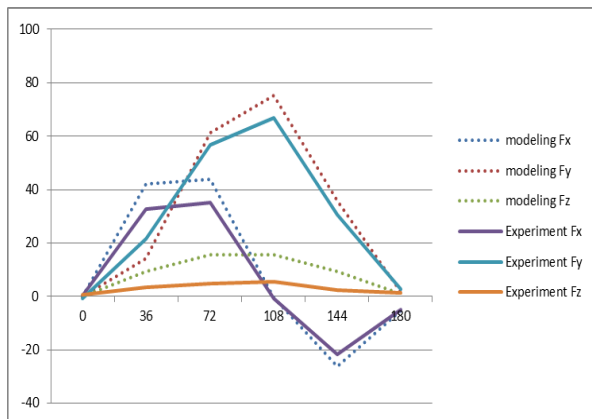
Θ	Cutting Force		
	F_x	F_y	F_z
0	0,0349416	-0,089799912	0
36	37,02647551	12,28680232	8,08412139
72	46,09296141	64,41472963	16,42646729
108	-0,57203901	79,20537391	16,42646729
144	-23,12725359	31,41744009	8,08412139
180	-6,022098336	1,981206024	1,303127503



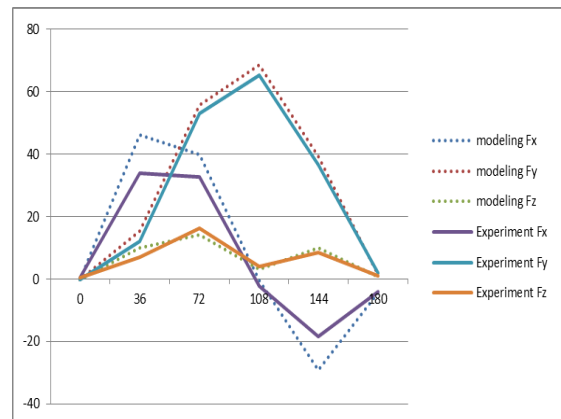
(a) Cutting force (N) versus a cutting speed of 18.84 m/min



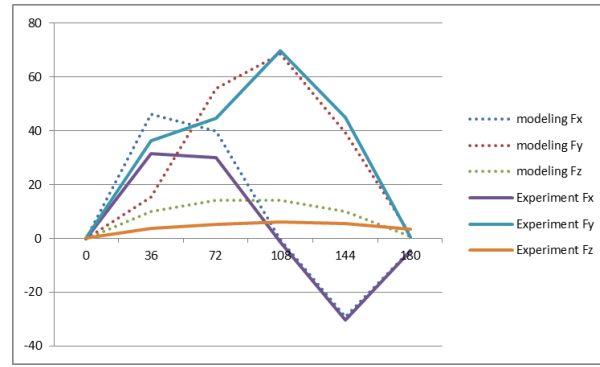
(b) Cutting force (N) versus a cutting speed of 21.84 m/min



(c) Cutting force (N) versus a cutting speed of 25.12 m/min



(d) Cutting force (N) versus a cutting speed of 28.26 m/min



(e) Cutting force (N) versus a cutting speed of 31.4 m/min

Figure 5. Cutting force graph from both experimental and modelling results

B. Effects of Cutting Speed on Cutting Force

By using the same method as described above, the cutting force of the tool on the PEEK material is also employed at various cutting speeds. This procedure is done to obtain the data differences from each difference in cutting speed in the rough machining process. In general, the optimum cutting speed is determined based on the tool's ability to obtain a short machining time. The cutting speed values used as the basis for comparison of cutting forces are 18.84, 21.98, 25.12, 28.26 and 31.4 m/min.

The cutting force regarding the F_x starts from the 0° cut angle, then 36° and multiples thereof. At an angle of 36° , the cutting force has almost the same value among the five cutting speed variations, where the largest cutting force value is 34.02 N at a cutting speed of 21.98 m/min, and the lowest cutting force value is 31.56 N at a cutting speed of 31.4 m/min. At a tool angle of 72° , the resulting

cutting forces have different values. At this angle, the greatest cutting force value is 39.73 N at a cutting speed of 18.84 m/min, and the lowest cutting force value is 21.88 N at a cutting speed of 21.98 m/min. At an angle of 108° , the entire cutting force at each cutting speed variation decreases. The lowest value of the cutting force at this angle is -17.14 N at a cutting speed of 21.98 m/min, and the highest value of the cutting force is 0.16 N at a cutting speed of 18.84 N. At an angle of 144° , all cutting speed used have a minus value, with the highest value of -14.9 N at a cutting speed of 21.98 m/min, and the lowest value of -30.26 N at a cutting speed of 31.4 m/min. At an angle of 180° , the cutting force resulting from the experimental results also has a low value; at this angle, the greatest value of the cutting force is 2.17 N at a cutting speed of 18.84 m/min, and the lowest value is -5.34 N at a cutting speed of 21.98 m/min.

The cutting force on F_y is shown in Fig. 6.

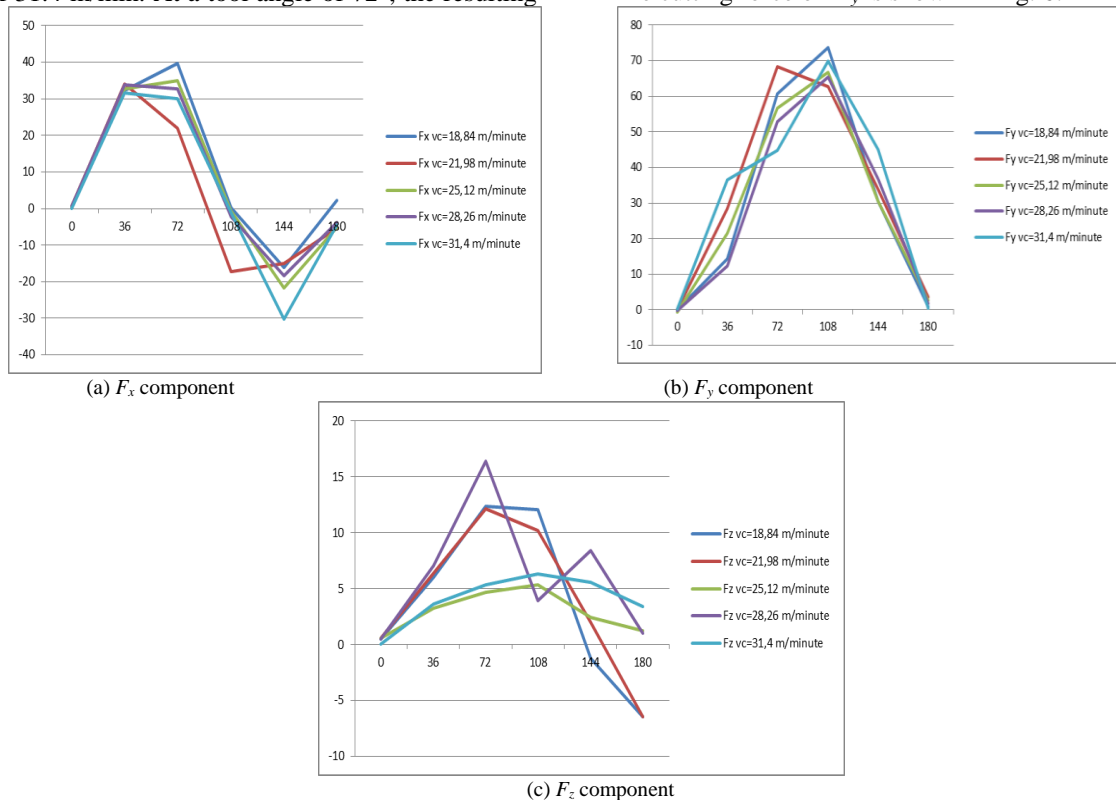
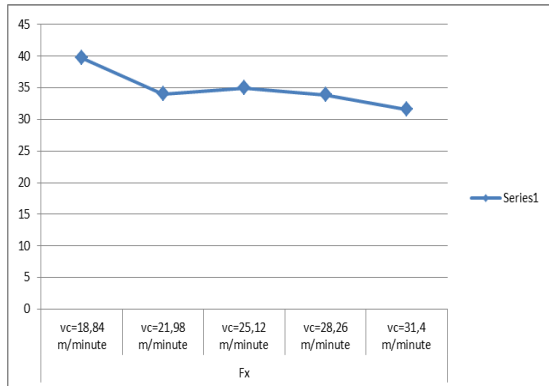


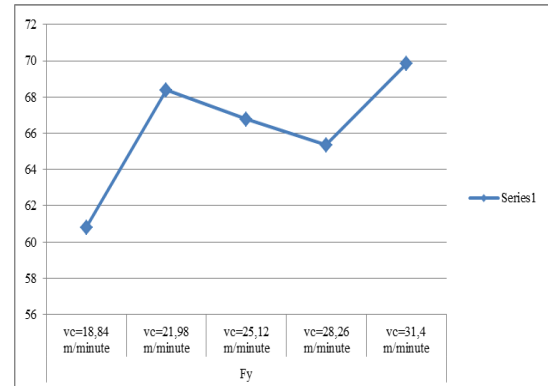
Figure 6. Cutting force results at different cutting speeds

As seen in the image above, when the cutting force is at an angle of 36° , the highest value is 7.09 N at a cutting speed of 28.26 m/min, and the lowest cutting force is 3.66 N at a cutting speed of 31.4 m/min. The largest difference in cutting force is at a loss angle of 72° , where the highest value is 16.4 N at a cutting speed of 28.26 m/min, and the lowest value is 4.68 N at a cutting speed of 25.12 m/min. At an angle of 180° , a minimum value of -6.48 N at a

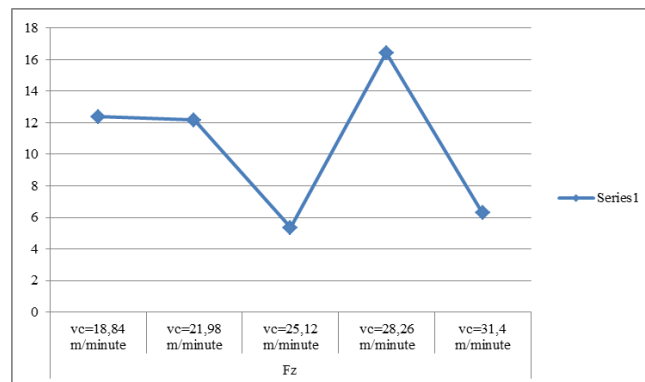
cutting speed of 18.84 m/min is observed, and the highest cutting force value is 3.41 N at a cutting speed of 31.4 m/min. The addition of the feed rate during the machining process implies a change in cutting speed, which further changes the cutting force. The highest cutting force at each cutting speed varies according to the component of the cutting force. The force components F_x , F_y and F_z are shown in Fig. 7.



(a) F_x component



(b) F_y component



(c) F_z component

Figure 7. Highest cutting force on each component

Based on the data generated in this study, the machining process using PEEK material obtains the highest cutting force value of 39.73 N on the F_x at a tool rotation of 72° and a cutting speed of 18.84 m/min. For F_y , the highest value is 73.74 N at a cutting speed of 18.84 m/min and a tool rotation angle of 108° . For F_z , the highest cutting force value is 16.43 N at a cutting speed of 28.26 m/min and a tool rotation angle of 72° .

IV. CONCLUSION

From the results above, when the feed rate changes during the machining process, the cutting speed also changes with the other parameters. The cutting force received by the tool on the work piece also fluctuates. At each turning angle of the tools, the magnitude of the cutting force at each cutter location point has a different magnitude. At a cutting speed value of 18.84 m/min, the largest cutting force value of 46,092 N at a rotation angle of 72° on the F_x component occurs. At the F_y component, at the tool rotation angle of 108° , a value of 79,205 N is

recorded. At the F_z component at a rotation angle of 72° and 108° and the difference in the angle of rotation of the tool at the same cutting speed, the amount of cutting force received by the tool is not always constant and tends to fluctuate. Likewise, for the difference in cutting speed, the higher the cutting speed value, the higher the decrease in cutting force. This finding indicates that a higher cutting speed produces a high cutting force value and creates a relatively large fluctuation in the force at each tool rotation angle at the end. This factor affects the tool's lifespan and other components of the machine. Thus, to avoid damage, the cutting force received by the tool against the object must be kept as constant as possible.

Given the large difference between the cutting force and the occurrence of vibration in the work piece, which allows harmonic motion, further research must be conducted.

CONFLICT OF INTEREST

The authors declare no conflict of interest.

ACKNOWLEDGMENT

This research was funded by the BLU funds of the Universitas Negeri Jakarta with the decision of the number 21/PUU/LPPM/IV/2021

REFERENCES

[1] Ü. A. Usca, M. Uzun, S. Şap, M. Kuntoğlu, K. Giasin, D. Y. Pimenov, *et al.*, "Tool wear, surface roughness, cutting temperature and chips morphology evaluation of Al/TiN coated carbide cutting tools in milling of Cu–B–CrC based ceramic matrix composites," *Journal of Materials Research and Technology*, vol. 16, pp. 1243–1259, 2022.

[2] Ü. A. Usca, S. Şap, M. Uzun, M. Kuntoğlu, E. Salur, A. Karabiber, *et al.*, "Estimation, optimization and analysis based investigation of the energy consumption in machinability of ceramic-based metal matrix composite materials," *Journal of Materials Research and Technology*, vol. 17, pp. 2987–2998, 2022.

[3] Ü. A. Usca, M. Uzun, M. Kuntoğlu, E. Sap, and M. K. Gupta, "Investigations on tool wear, surface roughness, cutting temperature, and chip formation in machining of Cu-B-CrC composites," *The International Journal of Advanced Manufacturing Technology*, vol. 116, pp. 3011–3025, October, 2021.

[4] E. Şap, U. A. Usca, M. K. Gupta, and M. Kuntoğlu, "Tool wear and machinability investigations in dry turning of Cu/Mo-SiCp hybrid composites," *The International Journal of Advanced Manufacturing Technology*, vol. 114, pp. 379–396, May, 2021.

[5] H. H. Sutrisno, G. Kiswanto, and J. Istiyanto, "Development of initial tool orientation method at close bounded area for 5-axis roughing based on faceted models," *International Journal of Mechanical Engineering and Robotics Research*, pp. 296–300, 2017.

[6] H. H. Sutrisno, G. Kiswanto, and J. Istiyanto, "The improvement of the Closed Bounded Volume (CBV) evaluation methods to compute a feasible rough machining area based on faceted models," *IOP Conference Series: Materials Science and Engineering*, vol. 215, p. 012041, 2017.

[7] G. Kiswanto, H. H. Sutrisno, and J. Istiyanto, "Non machinable volume calculation method for 5-Axis roughing based on Faceted models through closed bounded area evaluation," *MATEC Web of Conferences*, vol. 108, p. 04015, 2017.

[8] S. Braun, M. Storchak, and H. C. Mohring, "Using model based analytic cutting force prediction in CAM toolpath generation," *Procedia CIRP*, vol. 82, p. 6, 2019.

[9] T. Matsumura and S. Tamura, "Cutting force model in milling with cutter runout," *Procedia CIRP*, vol. 58, pp. 566–571, 2017.

[10] H. Hendriko, "Cut geometry calculation for the semifinish five-axis milling of nonstraight staircase workpieces," *Journal of Mechanical Science and Technology*, vol. 34, pp. 1301–1311, 2020.

[11] M. Schwenzer, S. Stemmler, M. Ay, T. Bergs, and D. Abel, "Continuous identification for mechanistic force models in milling," *IFAC Paper Online*, vol. 52-13, p. 6, 2019.

[12] A. N. Balasubramanian, N. Yadav, and A. Tiwari, "Analysis of cutting forces in helical ball end milling process using machine learning," *Materials Today: Proceedings*, 2020.

[13] M. Aydın and U. Köklü, "Analysis of flat-end milling forces considering chip formation process in high-speed cutting of Ti6Al4V titanium alloy," *Simulation Modelling Practice and Theory*, vol. 100, p. 102039, 2020.

[14] X. Liu, W. Wang, R. Jiang, Y. Xiong, K. Lin, J. Li, *et al.*, "Analytical model of cutting force in axial ultrasonic vibration-assisted milling in-situ TiB2/7050Al PRMMCs," *Chinese Journal of Aeronautics*, vol. 34, pp. 160–173, 2021.

[15] S. C. Huang, M. S. Chen, N. T. Nguyen, and Y. C. Kao, "A combination method of the theory and experiment in determination of cutting force coefficients in ball-end mill processes," *Journal of Computational Design and Engineering*, vol. 2, pp. 233–247, 2015.

[16] T. G. Molnar, S. Berezvai, A. K. Kiss, D. Bachrathy, and G. Stepan, "Experimental investigation of dynamic chip formation

in orthogonal cutting," *International Journal of Machine Tools and Manufacture*, vol. 145, p. 103429, 2019.

[17] G. C. Behera, J. Thrinadh, and S. Datta, "Influence of cutting insert (uncoated and coated carbide) on cutting force, tool-tip temperature, and chip morphology during dry machining of Inconel 825," *Materials Today: Proceedings*, vol. 38, pp. 2664–2670, 2021.

[18] S. Singh Bedi, S. Prasad Sahoo, B. Vikas, and S. Datta, "Influence of cutting speed on dry machinability of AISI 304 stainless steel," *Materials Today: Proceedings*, vol. 38, pp. 2174–2180, 2021.

[19] J. Wang, J. Zuo, Z. Shang, and X. Fan, "Modeling of cutting force prediction in machining high-volume SiCp/Al composites," *Applied Mathematical Modelling*, vol. 70, pp. 1–17, 2019.

[20] T. Kitamura, R. Tanaka, Y. Yamane, K. Sekiya, and K. Yamada, "Performance evaluation method for cutting fluids using cutting force in micro-feed end milling," *Precision Engineering*, vol. 62, pp. 232–243, 2020.

[21] S. Yamato and Y. Kakinuma, "Precompensation of machine dynamics for cutting force estimation based on disturbance observer," *CIRP Annals*, vol. 69, pp. 333-336, 2020.

[22] M. Wan, S. E. Li, H. Yuan, and W. H. Zhang, "Cutting force modelling in machining of fiber-reinforced polymer matrix composites (PMCs): A review," *Composites Part A: Applied Science and Manufacturing*, vol. 117, pp. 34-55, 2019.

[23] Y. He, J. Sheikh-Ahmad, S. Zhu, and C. Zhao, "Cutting force analysis considering edge effects in the milling of carbon fiber reinforced polymer composite," *Journal of Materials Processing Technology*, vol. 279, p. 116541, 2020.

[24] P. Parhad, V. Dakre, A. Likhite, and J. Bhatt, "The impact of cutting speed and depth of cut on cutting force during turning of austempered ductile iron," *Materials Today: Proceedings*, vol. 19, pp. 6630–669, 2019.

[25] X. Pang, Y. Zhang, C. Wang, Z. Chen, N. Tang, and B. Chen, "Effect of cutting parameters on cutting force and surface quality in cutting of articular cartilage," *Procedia CIRP*, vol. 89, p. 6, 2020.

[26] M. A. Rubeo and T. L. Schmitz, "Mechanistic force model coefficients: A comparison of linear regression and nonlinear optimization," *Precision Engineering*, vol. 45, pp. 311–321, 2016.

Copyright © 2022 by the authors. This is an open access article distributed under the Creative Commons Attribution License (CC BY-NC-ND 4.0), which permits use, distribution and reproduction in any medium, provided that the article is properly cited, the use is non-commercial and no modifications or adaptations are made.



Himawan Hadi Sutrisno was born in Blitar, East Java Province, Indonesia. He graduated on 2005 with a Bachelor's degree in Mechanical Engineering, Major in Manufacturing at the Brawijaya University. The author completed his Master's degree studies on 2008 at the Universitas Indonesia in Depok and took his Doctorate degree in the same university as the Mechanical Engineering Department and Manufacturing concentration. The author graduated in 2018 with honours and is currently

continuing his expertise.

The author works as a researcher in the Manufacturing Field of the Fire, Material and Safety Laboratory at Universitas Negeri Jakarta, Indonesia. In this field, knowledge regarding the manufacturing industry is developed for production technology and safety production. At present, the author is a consistent contributor to these two fields, with several publications in the fields of 5-axis milling, manufacturing, materials and fire safety.

Dr. Ir. Himawan Hadi Sutrisno, ST, MT, has intellectual property rights in the development of a firefighter motorcycle issued by the Ministry of Law and Human Rights of the Republic of Indonesia.